Available online at www.sciencedirect.com

ScienceDirect

Procedia Engineering 13 (2011) 88–93

Engineering Procedia

5th Asia-Pacific Congress on Sports Technology (APCST)

Methods for evaluating the radial structural behaviour of racing bicycle wheels

Nicola Petrone*, Federico Giubilato

Department of Mechanical Engineering, University of Padova, Via Venezia 1, 35131 Padova, Italy

Received 20 March 2011; revised 14 May 2011; accepted 16 May 2011

Abstract

Aim of the work was the development of a test method for evaluating the radial structural behaviour of racing wheels, believed to be correlated with the riding comfort properties. Four front wheels of different shape, material and spoke disposition were equipped with the same tubular tires and tested under radial loads. The wheel/rim/tire load-displacement curves were measured in static, cyclic and bump tests. The stiffness varied with load: despite great differences in the rim behaviour, the wheel overall behaviour resulted very similar due to the tire masking effect.

Keywords: Racing bicycle; wheels; radial loads; stiffness; static; dynamic

1. Introduction

The perceived quality of a racing wheel is related to the combination of several performance parameters with the level of comfort during long cycling tracks on irregular road textures. Cruising comfort is related to the radial behaviour of the wheel assembly, intended as combination of tire and rim. Radial properties of wheels are believed to be dependent on tire pressure and construction, rim profile and materials, spoke design and disposition, hub shape and materials.

Despite the common opinion among cyclists that the wheel radial properties affect the rider's back comfort, previous studies were focusing mainly on the effects of rider's weight (Stone & Hull [1]) or on the frame materials (Hastings *et al.* [2]). Very few studies were analyzing the structural radial behaviour of wheels and their correlation with the degree of rider's comfort. The aim of the present work was the

* Corresponding author. Tel.: +39-049-8276761; fax: +39-049-8276785.
E-mail address: nicola.petrone@unipd.it.

1877–7058 © 2011 Published by Elsevier Ltd.
doi:10.1016/j.proeng.2011.05.056

development of a standard test method for the quantitative analysis of racing wheels in terms of static and dynamic radial behaviour.

2. Materials

Four front racing wheels (named AF, BF, CF, DF) were selected for the study. Wheels were all equipped with the same tubular tire (Continental "Sprinter" 700x23) inflated at 8 bar, but were different for material, rim profile, spokes number and disposition as summarized in Table 1.

Table 1. Tested wheels characteristics (* mass including tire).

Wheel	Rim profile	Rim material	Hub material	Spokes Nr. Front	Spokes Pattern Front	Spokes material	Mass* Front
AF	Low H 20 mm	Composite	Composite	22	Radial	Steel	850 g
BF	High H 50 mm	Aluminium	Aluminium	18	Radial	Steel	900 g
CF	Medium H 30 mm	Composite	Composite	20	2x	Composite	760 g
DF	Medium H 30 mm	Aluminium	Aluminium	16	Radial	Steel	930 g

The wheels were rigidly supported at the hub axis as shown in Figure 1(a): A servohydraulic MTS 242 cylinder with a 15 kN load cell was used to load the wheels in the radial direction by means of a stiff aluminium plate (Figure 1(b)). The load was applied to the tire and the radial displacement of the wheel system x_W was measured by the cylinder's internal LVDT. An additional LVDT was placed internally on the rim to measure the rim radial displacement x_R: the tire radial compression x_T was calculated as the difference between the wheel and the rim displacements.

The Wheel assembly was considered as the combination of two subsystems, as shown in Figure 1(c): The Rim subsystem (composed by rim, spokes and hub) and the Tire subsystem. The Wheel system resulted to be composed by tire, rim, spokes and hub. The wheel system was modelled by a lumped parameters model (Figure 1(c)) composed by 2 subsystems in series (spring-damper parallel elements) representing respectively the 2 subsystems Rim and Tire.

3. Methods

Three types of radial tests were developed, having different maximum load levels and different loading rates: Static, Cyclic and Bump tests. In the Static radial test the maximum load of 2000 N was reached at a loading rate of 200 N/s (Figure 2(a)): the rational of this test was the simulation of a quasi-static radial overload on the wheel. The Cyclic radial test was developed in order to simulate the load acting on the wheel during its rolling over a flat and smooth surface at a speed of 30 km/h. It consisted in the repeated application at 4 Hz frequency of the load cycle shown in Figure 2(b), composed by a half sine load reaching the peak of 1000 N and a zero load plateau of the same duration. The maximum load rate was about 14800 N/s. The Bump test was introduced to simulate the case when the wheel hits a common obstacle like a road bump. The maximum load of 1500 N was linearly reached at a constant loading rate

of 22200 N/s (Figure 2(c)). In the cyclic and the bump tests, both the radial stiffness and the energy dissipated by the wheels were evaluated.

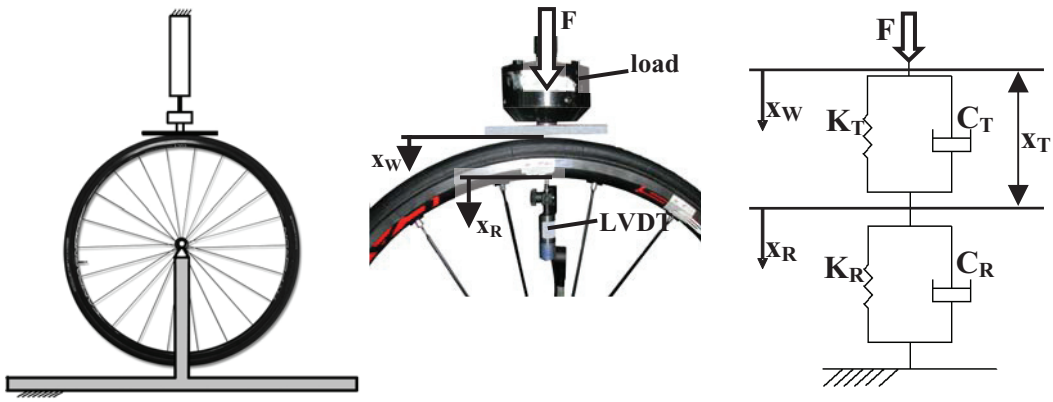

Fig. 1. (a) Schematics of the test bench. (b) Measuring system. (c) Lumped parameters model.

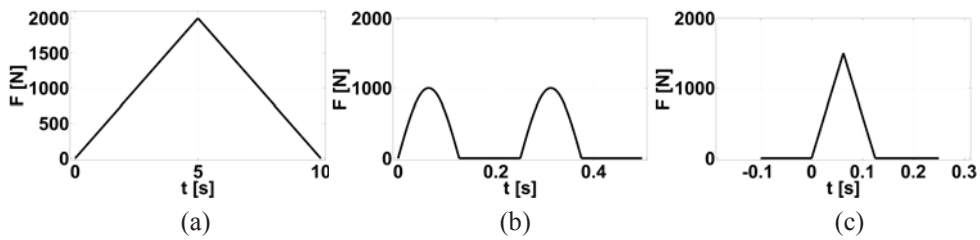

Fig. 2. (a) Load function applied during static tests. (b) Cycle repeated during cyclic tests. (c) Load function applied during bump tests.

All tests were performed with the same tubular tires inflated at 8 bar and controlled by a precision pressure gauge. Spokes pre-tension levels were not measured, nor the spokes tension throughout the tests. The effect of tire pressure was investigated by performing pilot static tests on the same front wheel AF with the tubular inflated at 7, 8 and 9 bar. The Load-Displacement curves obtained were recorded at 2 kHz during all the three types of tests and further analyzed in order to calculate meaningful values of the stiffness K (N/mm), defined as the local tangent slope to the Load-Displacement curves. The stiffness K was evaluated for Wheel (K_W), Rim (K_R) and Tire (K_T): due to the nonlinearity of the wheel assembly behaviour, the stiffness values varied with the load level and were plotted as a function of the applied load F. For each subsystem, the calculation of stiffness K was performed at load steps of 100 N, based only on the raising part of the load cycle as represented in the load-displacement diagram (Figure 3(a)). A second letter in the subscript was introduced to distinguish among Static (S), Cyclic (C) and Bump (B) test results. From the static tests data, a critical load P_{cr} of the wheel was also calculated in the cases showing sudden rim stiffness decrease ΔK_{RS} greater than 20%. In addition, a linear least squares fitting of the complete load cycle was performed in order to calculate the overall cycle stiffness value K^C (Figure (3b)): the scatter from a linear behaviour was expressed by the R^2 parameter. With respect to Cyclic and Bump tests, the energy E dissipated by the three subsystems was calculated as the area enclosed between the

increasing and decreasing load branches of the load cycle, after introduction of a minimum threshold of 50 N - cyclic tests - or 200 N - bump tests (Figure 3(c)).

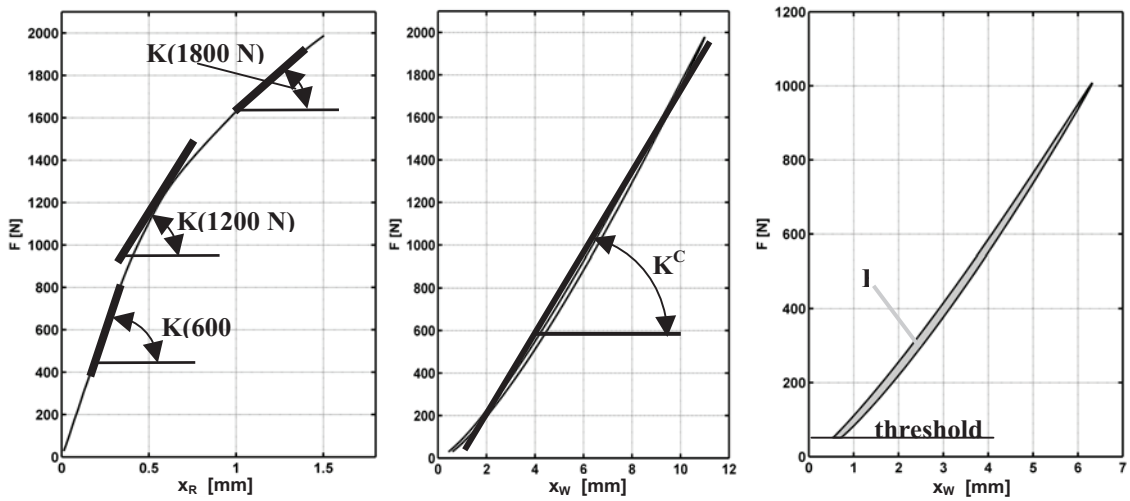

(a) (b) (c)

Fig. 3. (a) Example of a Load-Displacement curve and calculation of local stiffness K as a function of load. (b) Calculation of the cyclic stiffness parameter K^C. (c) Representation of the cyclic dissipated energy E.

4. Results and Discussion

The results of the Static, Cyclic and Bump tests performed on Front wheels are reported in Figure 4 and Tables 2 - 4. The curves of the Static Stiffness as a function of load for the four Front wheels are reported in Figure 4(a) and can be compared with the rim stiffness curves, Fig 4(b). Despite the rim stiffness resulted to differ of more than a factor of four within the tested wheels (ranging from 811 N/mm, rim C, to 3681 N/mm, rim B), the wheel assembly behaviour resulted to be very similar (ranging from 179 N/mm, wheel C, to 200 N/mm, wheel B). This tendency was also confirmed by the Cyclic Stiffness curves for the four Front wheels (Figure 4(c)) and rims (Figure 4(d)) and by the Bump Stiffness curves for the four Front wheels (e) and rims (f). The rim stiffness values during static tests tended to be constant with increasing loads, except for rim CF that revealed an evident unstable behaviour of spokes at loads greater than 1000 N, when it lost almost the 68 % of its stiffness. This instability phenomenon is related to spokes axial stress changing from tension to compression at P_{cr}, possibly due to low pre-tensioning levels, as showed by video images. The spokes pre-tension determines the overall load at which critical spokes can change from tensile to compression stresses, therefore causing a global unstable behaviour. The flatness of Rim stiffness curves up to the critical load P_{cr} suggests that Rim stiffness is not influenced by spokes pre-tension levels: this fact may need further confirmation by tests performed measuring also spokes tension.

Linearity of rim stiffness static curves induced to attribute mostly to tires the nonlinear shape of wheel stiffness curves. Nevertheless, the comparison of rim stiffness curves (Figure 4(b), (d), (f)) showed the appearance of nonlinear stiffness behaviour of B & C rims during the cyclic and bump tests, thus suggesting a more detailed analysis of the deflection behaviour of such rims. In general, the wheel assembly stiffness resulted to decrease with increasing load rate (Figure 4(a), (c), (e)): the stiffness curve during bump tests was non-monotonic, showing a relative peak around 1000 N. The effect of the inflation pressure on the wheel stiffness curve for the Front wheel A is presented in Figure 4(g). The equivalent

behaviour of the tire obtained from different wheels during the dynamic bump tests (Figure 4(h)) was assumed as a validation of the test method and the overall approach. This fact was suggesting also the possibility of studying the tire stiffness and damping properties using the present approach.

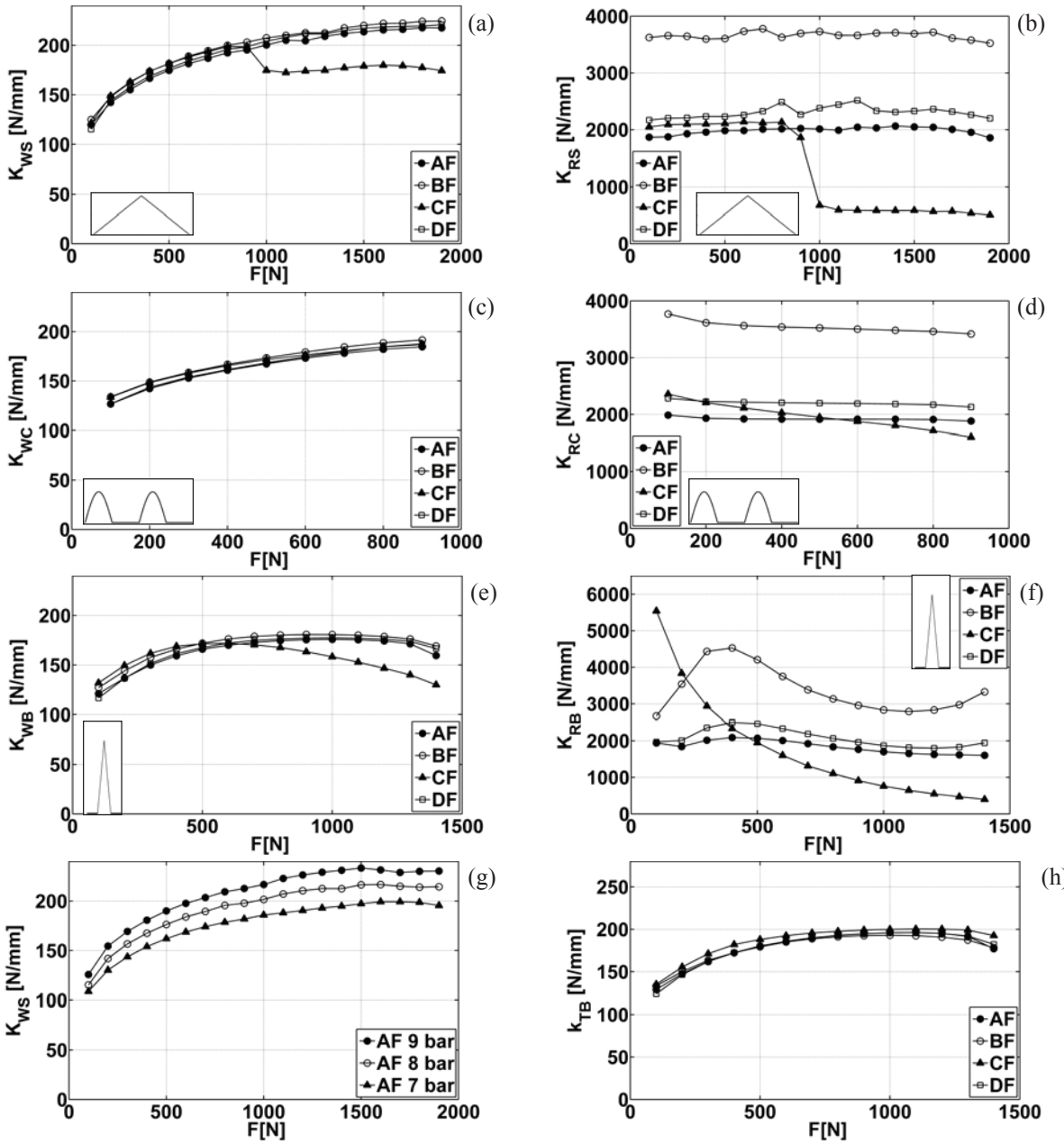

Fig. 4. Results of Static, Cyclic and Bump tests. (a-b) Static stiffness curves as a function of load for the four Front wheels (a) and rims (b). (c-d) Cyclic stiffness curves for the four Front wheels (c) and rims (d). (e-f) Bump stiffness curves for the four Front wheels (e) and rims (f). (g) Inflation pressure effect on the wheel stiffness curve for the front wheel A. (g) Tire stiffness curves from the four wheels after bump tests.

Table 2. Results of Front wheels Static tests.

WHEEL	$K_{WS}{}^{C}$ [N/mm]	$R^2(K_{WS}{}^{C})$	$K_{RS}{}^{C}$ [N/mm]	$R^2(K_{RS}{}^{C})$	P_{CR} [N]	ΔK_{RS} at P_{CR} [%]
AF	193	0.9941	2007	0.9988	> 2000	-
BF	200	0.9944	3681	0.9983	> 2000	-
CF	179	0.9980	811	0.9327	1000	-68
DF	196	0.9936	2341	0.9980	> 2000	-

Table 3. Results of Front wheels Cyclic tests.

WHEEL	$K_{WC}{}^{C}$ [N/mm]	$R^2(K_{WC}{}^{C})$	$K_{RC}{}^{C}$ [N/mm]	$R^2(K_{RC}{}^{C})$	E_{WC} [J]	E_{RC} [J]
AF	166	0.9948	1926	0.9987	162	13
BF	173	0.9951	3544	0.9986	158	7
CF	171	0.9952	1927	0.9962	168	15
DF	168	0.9945	2202	0.9990	167	10

Table 4. Results of Front wheels Bump tests.

WHEEL	$K_{WB}{}^{C}$ [N/mm]	$R^2(K_{WB}{}^{C})$	$K_{RB}{}^{C}$ [N/mm]	$R^2(K_{RB}{}^{C})$	E_{WB} [J]	E_{RB} [J]
AF	159	0.9905	1811	0.9947	532	61
BF	165	0.9906	3284	0.9933	543	35
CF	152	0.9910	935	0.9356	681	180
DF	161	0.9896	2056	0.9946	547	52

5. Conclusions

A new methodology for evaluating the radial structural properties of racing bicycle wheels was proposed: the constant behaviour of the tire obtained from different wheels during the dynamic bump tests was assumed as a validation of the test method. The work showed that high differences in rim stiffness were not corresponding to great variations of the wheel assembly radial stiffness at a typical cycling pressure of 8 bar. The tire stiffness was able to mask the rim differences, thus involving further detailed analysis of the perceived wheel comfort behaviour on the road and its correlation with the wheel structural parameters.

References

[1] Stone C., Hull M.L., Effect of rider weight on rider-induced loads during common cycling situations, Journal of Biomechanics, 28 (4), 365-375.

[2] Hastings A.Z., Blair K.B., Culligan F.K., Pober D.M., Measuring the effect of transmitted road vibration on cycling performance, The Engineering of Sport 5, Davis, 2004.